Advanced Engineering Forum *Online: 2011-12-22*
ISSN: 2234-991X, Vols. 2-3, pp 366-371
doi:10.4028/www.scientific.net/AEF.2-3.366

Dynamic Analysis of a 165Kg Spot Welding Robot

Li Cheng[a],Yuwang Liu[b], Hongguang Wang[c], Yong Chang, Yifeng Song and Haitao Luo

The State Key Laboratory of Robotics, Shenyang Institute of Automation, CAS, China

[a]chengli@sia.cn, [b]liuyuwang@sia.cn, [c]hgwang@sia.cn

Keywords: Spot welding robot, Heavy payload, Dynamics, Simulation

Abstract. A novel 165Kg spot welding robot is introduced, which is independently developed by China. The Newton-Euler approach is used to derive the dynamic equation. Then, entity model of the robot is built up with Solidworks software. The motion of the robot is planned by the position, velocity and acceleration of all the joint. The first three joints, which bear most of the payload and the own weight of the robot, are set with maximum acceleration during the accelerating/ decelerating process. According to the planned trajectory, dynamic simulation is carried out using Solidworks. The driving torques of each joint are obtained. From the dynamic analysis, we find the position yielding the maximum driving torque while the robot is moving with the maximum payload and the maximum speed. The moment of inertia is a predominant influence in the causation of big actuating torque.

Introduction

Industrial robots with high payload, high speed and high precision are urgently demanded in advanced manufacture fields, ranging from welding, painting, material handling and assembly to cutting [1]. They have become indispensable for achieving productivity and flexibility in fully automated production lines. To improve their performance, many researchers have discussed the kinematics [2], dynamics [3, 4], and trajectory optimization [5], and structural optimization [6], modal analysis and so on [7, 8].

Although many scholars have done a lot of research on industrial robot, dynamics is still a key element and hot topic in these developments, especially for the industrial robots with heavy payload [9,10] and high speed. As a consequence, with 165Kg spot welding robot as an example, this paper introduces the procedure of dynamic modeling and simulation analysis of six-revolute industrial serial robots. Firstly, the SRD 165A spot welding robot is introduced. Secondly, dynamic formulation of the robot is derived by Newton-Euler approach. Then, the assembly model of the robot is established with Solidworks. The motion of the robot is planned by the position, velocity and acceleration of all the joint. Finally, according to the planned trajectory, dynamic simulation is carried out with the maximum 165Kg payload attached to the end of the manipulator.

Description of the 165Kg Spot Welding Robot

The SRD 165A spot welding robot is shown in Fig. 1, which is independently developed by China recently. The total weight of this robot is 1400Kg, while the maximum payload is 165Kg. It is an articulated manipulator with six revolute joints. The waist, shoulder and elbow joints are driven by motors through RV reducer respectively, meeting the requirements of high rigidity and large torque; the three-orthogonal-axis wrist joints are driven by motors through a certain number of gear groups of deceleration and harmonic reducer respectively, satisfying the requirements of light weight and high precision. For the first three joints, the driving motors are placed near each joint and the output shafts of the motors are connected to the RV reducers to make the links rotate directly. For the joint 4, joint 5 and joint 6 of the wrist, the driving motors are placed at the end of fore arm to ensure the less mass of the wrist. The spring balancer is adopted to reduce the biased load delivered to the driving motor on shoulder joint. Fig. 2 shows the robot mechanism diagram and the coordinate system of robot links.

Fig. 1. SRD 165A spot welding robot

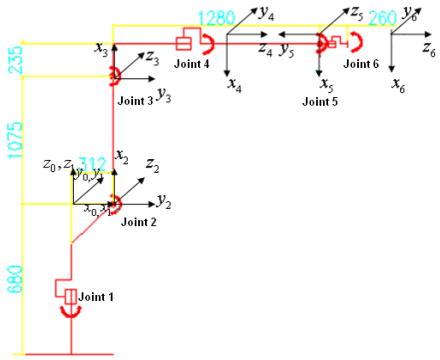

Fig. 2. The coordinate system of robot links

Dynamic Formulation

Dynamics of mechanism defines the relationship between the motion of the robot and the actuator torques. In this section, Newton-Euler approach is used to derive the dynamic equation.

Velocities and Accelerations. The linear and angular accelerations of each link should be obtained first. The joint angular velocity is described as $\dot{\boldsymbol{q}}=[\dot{\theta}_1 \quad \dot{\theta}_2 \quad \dot{\theta}_3 \quad \dot{\theta}_4 \quad \dot{\theta}_5 \quad \dot{\theta}_6]^{\mathrm{T}}$. ${}^{i}\boldsymbol{\omega}_i$ and ${}^{i}\dot{\boldsymbol{\omega}}_i$ are the vectors of angular velocity and angular acceleration of link i described in link frame $\{i\}$ respectively. ${}^{i}\dot{\boldsymbol{v}}_i$ and ${}^{i}\dot{\boldsymbol{v}}_{Ci}$ are the linear accelerations of the origin of frame $\{i\}$ and the centroid of link i expressed in frame $\{i\}$, respectively. Then the velocities and accelerations of each robot link (i=1,2,$\cdots$,6) can be derived through Newton-Euler recurrence formulas, listed as Eq. (1) to Eq. (4).

$$ {}^{i}\boldsymbol{\omega}_i = {}_{i-1}^{i}\boldsymbol{R}\,{}^{i-1}\omega_{i-1} + \dot{\theta}_i\,{}^{i}\hat{\boldsymbol{Z}}_i \tag{1} $$

$$ {}^{i}\dot{\boldsymbol{\omega}}_i = {}_{i-1}^{i}\boldsymbol{R}\,{}^{i-1}\dot{\boldsymbol{\omega}}_{i-1} + {}_{i-1}^{i}\boldsymbol{R}\,{}^{i-1}\boldsymbol{\omega}_{i-1}\times\dot{\theta}_i\,{}^{i}\hat{\boldsymbol{Z}}_i + \ddot{\theta}_i\,{}^{i}\hat{\boldsymbol{Z}}_i \tag{2} $$

$$ {}^{i}\dot{\boldsymbol{v}}_i = {}_{i-1}^{i}\boldsymbol{R}\,[{}^{i-1}\dot{\boldsymbol{\omega}}_{i-1}\times{}^{i-1}\boldsymbol{P}_i + {}^{i-1}\boldsymbol{\omega}_{i-1}\times({}^{i-1}\boldsymbol{\omega}_{i-1}\times{}^{i-1}\boldsymbol{P}_i) + {}^{i-1}\dot{\boldsymbol{v}}_{i-1}] \tag{3} $$

$$ {}^{i}\dot{\boldsymbol{v}}_{Ci} = {}^{i}\dot{\boldsymbol{\omega}}_i\times{}^{i}\boldsymbol{P}_{Ci} + {}^{i}\boldsymbol{\omega}_i\times({}^{i}\boldsymbol{\omega}_i\times{}^{i}\boldsymbol{P}_{Ci}) + {}^{i}\dot{\boldsymbol{v}}_i \tag{4} $$

where ${}_{i-1}^{i}\boldsymbol{R}$ describes the rotation of frame $\{i\text{-}1\}$ relative to frame $\{i\}$, which can be got through kinematics analysis. ${}^{i}\hat{\boldsymbol{Z}}_i$ is the unit vector of $\boldsymbol{Z}$-axis in frame $\{i\}$. ${}^{i-1}\boldsymbol{P}_i$ is the positional vector of origin of frame $\{i\}$ described in frame $\{i\text{-}1\}$. ${}^{i}\boldsymbol{P}_{Ci}$ is the positional vector of the centroid of link i expressed in frame $\{i\}$

The Force and Torque Acting on the link. After compute the linear and angular accelerations of the centroid of each link, the next step is to compute the inertia force and torque acting on each link (i=1,2,$\cdots$,6). According to Newton' equation, the force ${}^{i}\boldsymbol{F}_{Ci}$ can be computed by Eq. (5).

$$ {}^{i}\boldsymbol{F}_{Ci} = m_i\,{}^{i}\dot{\boldsymbol{v}}_{Ci} \tag{5} $$

where m_i is the total mass of link i.

The moment of inertia of link i can be calculated by Eq. (6)

$$ {}^{i}\boldsymbol{N}_{Ci} = {}^{Ci}\boldsymbol{I}_i\,{}^{i-1}\dot{\boldsymbol{\omega}}_{i-1} + {}^{i}\boldsymbol{\omega}_i\times({}^{Ci}\boldsymbol{I}_i\,{}^{i}\boldsymbol{\omega}_i)\,. \tag{6} $$

where ${}^{Ci}\boldsymbol{I}_i$ is the inertia tensor of link i .

Joint Torques. Having computed the accelerations and inertia forces acting on each link, the joint actuating torques will be calculated through Eq. (7) and Eq. (8).

$$ {}^{i}\boldsymbol{f}_{i} = {}^{i}_{i+1}\boldsymbol{R}\,{}^{i+1}\boldsymbol{f}_{i+1} + {}^{i}\boldsymbol{F}_{Ci} \tag{7} $$

$$ {}^{i}\boldsymbol{n}_{i} = {}^{i}\boldsymbol{N}_{Ci} + {}^{i}_{i+1}\boldsymbol{R}\,{}^{i+1}\boldsymbol{n}_{i+1} + {}^{i}\boldsymbol{P}_{Ci} \times {}^{i}\boldsymbol{F}_{Ci} + {}^{i}\boldsymbol{P}_{i+1} \times {}^{i}_{i+1}\boldsymbol{R}\,{}^{i+1}\boldsymbol{f}_{i+1} \tag{8} $$

where ${}^{i}\boldsymbol{f}_{i}$ is the force exerted on link i and ${}^{i}\boldsymbol{n}_{i}$ is the torque exerted on link i (i=6,5,$\cdots$,1).

Then the joint actuating torques can be found by taking the $\hat{\boldsymbol{Z}}$ component of the torque, described as Eq. (9).

$$ \boldsymbol{\tau}_{i} = {}^{i}\boldsymbol{n}_{i}\,{}^{i}\hat{\boldsymbol{Z}}_{i} \tag{9} $$

Now, the dynamic formulation has been derived by Newto-Euler equation. However, the calculation of dynamics becomes complex when the degree of freedom of the robot $n > 2$. Fortunately, dynamic simulation provids a simple way to study the dynamics of the robot. We will introduce it in detail in the following parts.

Dynamic Simulation

Dynamic simulation is an important procedure to investigate the dynamic characteristic of the heavy payload robot. Solidworks software is adopted for the dynamic simulation of this spot welding robot. First of all, the simplified entity model of the robot is built up. It is assembled with eight rigid parts, including the fixed base, link 1 to link 6 and the spring balancer, as shown in Fig.3 . The material of the base and the first three links is QT450, and the one of the wrist is cast steel. All the parts are regarded as rigid body with mass characteristics only. The adjacent components are connected through revolute joint. The spring balancer on joint 2 is set with the spring stiffness coefficient k=100N/mm, and the initial length of the spring is 128.2mm.The vertically highest posture is set as initial pose. Then, the motion of the robot is planned. At last, the dynamic simulation is carried out.

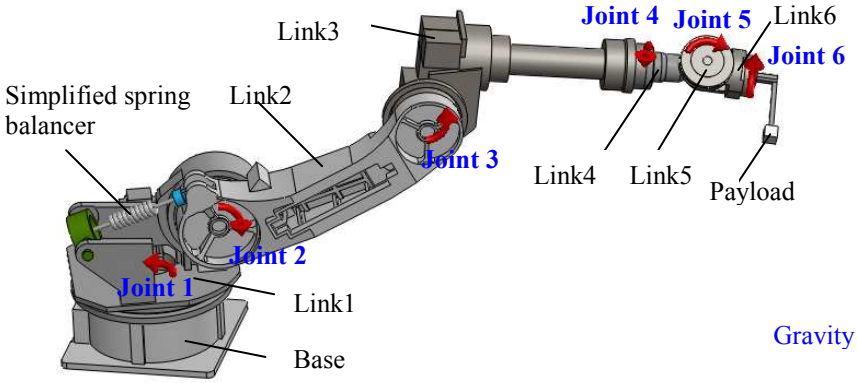

Fig. 3. Assembled model of the spot welding robot

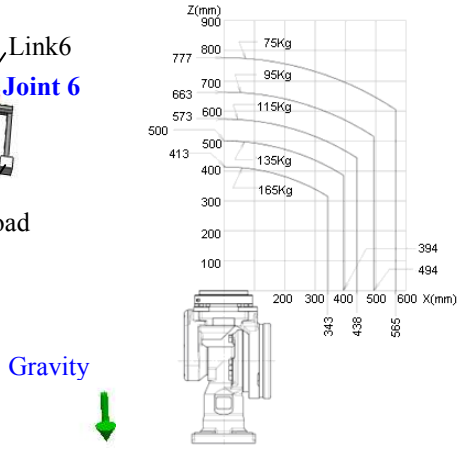

Fig. 4.Wrist load diagram of the spot welding robot

Load Input. The wrist load diagram of the spot welding robot is described in Fig. 4. In order to investigate the dynamic characteristic of 165Kg spot welding robot under bad working condition, the maximum payload of 165Kg is attached to the point (300,0, 300) in the wrist frame (unit: mm).

Motion Planning. The motion of the spot welding robot is planned by the position, velocity and acceleration of all the joint. The first three joints, which bear most of the payload and the deadweight of the robot, are set with maximum acceleration during the accelerating/ decelerating process. Fig. 5 shows the angular velocities of joint 1, joint 2 and joint 3, respectively. The motion of the wrist joints are set with sine function, as shown in Eq (10). According to this planned motion, the robot satisfies the following requirements: the joint 1 and joint 2 can reach the whole joint space during the given movement time; at time t =1.4s, the robot moves to the forward maximum horizontal state, as shown in Fig. 3; at time t = 4.2s, the robot moves to the reverse maximum horizontal position, as shown in

Fig. 6. In these two positions, joint 2 and joint 3 are both in accelerating/ decelerating state and the spot welding robot is in bad working configuration due to the cantilevered structure with severe dynamic condition.

$$\begin{cases} \dot{\theta}_4 = 110\sin(t) \\ \dot{\theta}_5 = 47.1\sin(2\pi t) \\ \dot{\theta}_6 = 150\sin(t + 2\pi/3) \end{cases} \tag{10}$$

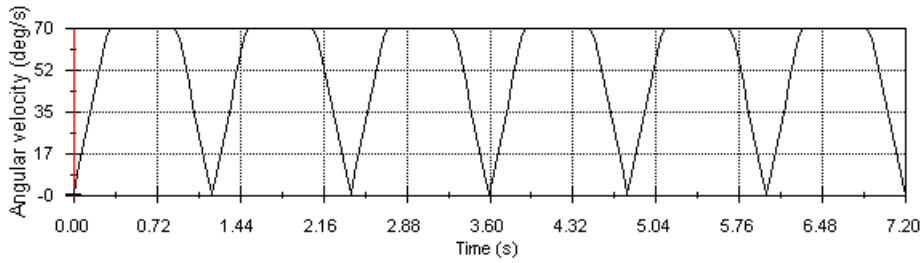

(a) Angular velocity of joint 1

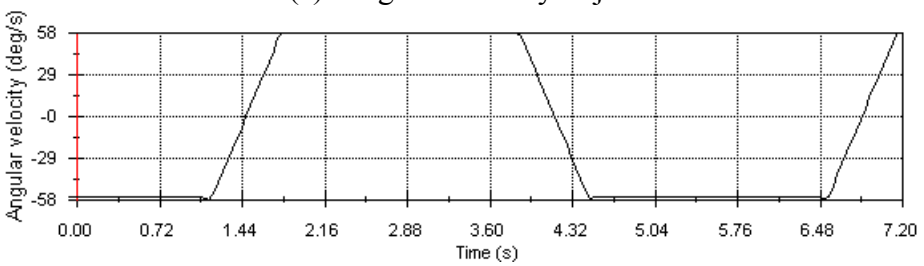

(b) Angular velocity of joint 2

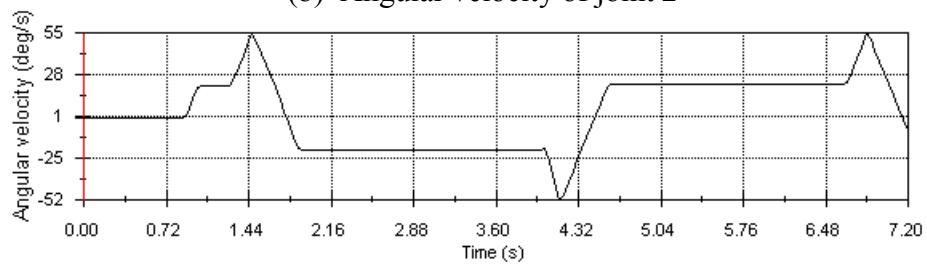

(c) Angular velocity of joint 3

Fig. 5. Angular velocity changing curves of each revolute joint

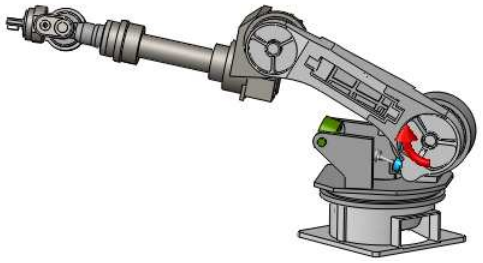

Fig. 6. Posture of the spot welding robot at time 4.2s

Dynamic Simulation Result. Rigid body dynamic simulation is performed following the planned motion in above section. The corresponding driving torques of each joint expressed in the link frame obtained from the simulation are illustrated in Fig. 7.

From the dynamic simulation, the position yielding the maximum driving torque can be found while the robot is moving with the maximum payload and the maximum speed. From the curves in Fig. 7, it can be seen that first three joints bear great torques which resulted by the heavy payload and the deadweight of all the links. The torque of wrist joints is relatively small. The positions at time 1.4s and 4.2s are the particular weak points because of large joint torques.

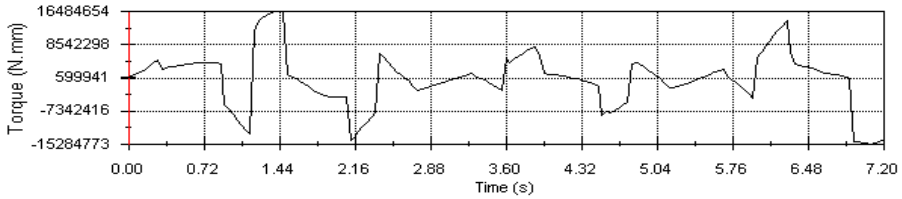

(a) Joint 1

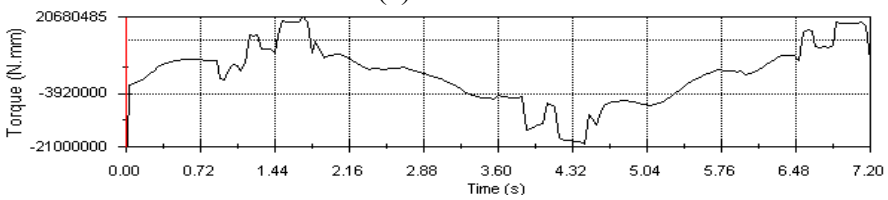

(b) Joint 2

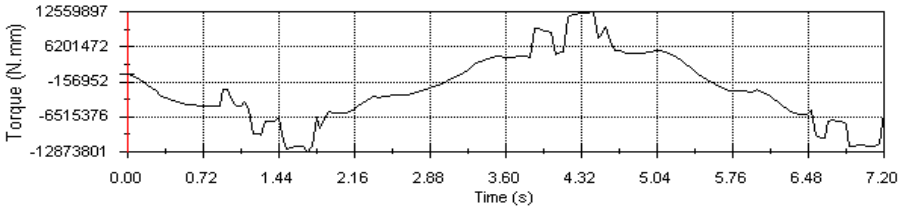

(c) Joint 3

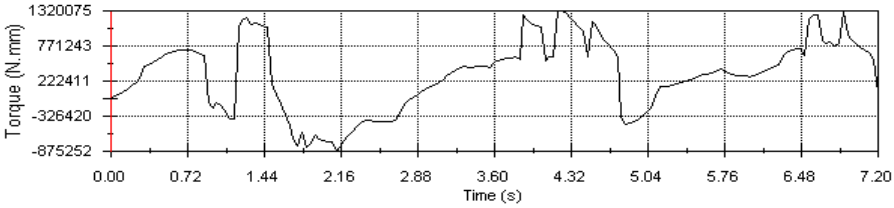

(d) Joint 4

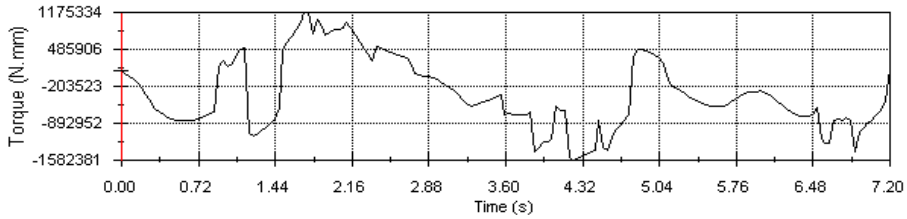

(e) Joint 5

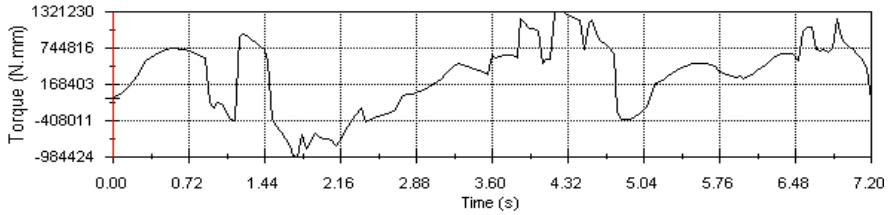

(f) Joint 6

Fig. 7. The torque of each revolute joint

Furthermore, the moment of inertia is a predominant influence in the causation of large actuating torque. For example, the driving torque of joint 2 is close to 20000Nm at time= 4.2s. At this moment, the robot moves to the reverse maximum horizontal position. The joint torque produced by the gravity of the payload and the links is about 5000Nm. It is only about 25% of the total driving torque. That is to say, the influence of the inertia force nearly comes to 70%~75%.At time =1.4s, the driving torque of joint 1 approaches to 17000Nm. This is also due to the maximum cantilevered configuration and the large instantaneous inertia.

It should be noticed that, for the purpose of great efficiency and speed of the dynamic simulation, the assembled model has not considered the effect of reducer in the transmission chains on each revolute joint. Thus, the driving torque obtained above should be converted to the one on driving motors according to the reduction ratio at all levels.

The spring force exerted on joint 2 by the spring balancer is described in Fig. 8. It changes along with the angle of joint 2 automatically.

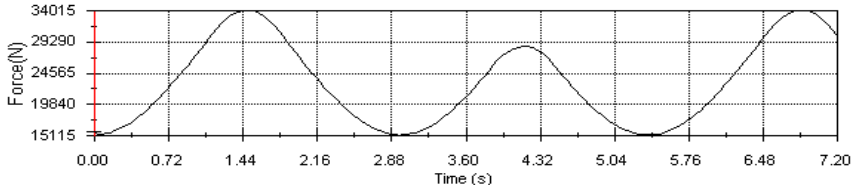

Fig. 8. The spring force of the balancer

Conclusion

Dynamics of 165Kg spot welding robot is analyzed in detail. The motion is planned which is helpful to find the weak point of the robot in the workspace. The magnitude and direction of the maximum actuating torque during the robot movement is found from dynamic simulation with Solidworks. This can provide guidance for the motor selection. In addition, it also lays the foundation for further stress distribution and deformation analysis under bad working condition and structural optimization design.

Acknowledgement

This work is supported by the National Science and Technology Major Project on High Grade CNC Machine Tool and Fundamental Manufacturing Equipment, China (Grant No. 2009ZX04013).

References

[1] Jan Swevers, Walter Verdonck, and Joris De Schutter. Dynamic Model Identification for Industrial Robots, IEEE Control Systems Magazine, 27(5), 2007: 58-71

[2] Zhang Xingguo, Xu Haili. Analysis on Struture and Kinematics of FANUC M-6iB Industrial Robot. Journal of Nantong University (Natural Science Edition), 8(1), 2009:9-12.

[3] Rafael M. Inigo, James S. Morton. Simulation of the Dynamics of an Industrial Robot, IEEE TRANSACTIONS on Education, 34(1), 1991: 89-99.

[4] Li Qingling, Zhao Yongsheng. Dynamic Analysis and Simulation of 6-DOF Industrial Robot, Journal of Shanghai Dianji University, 11(4), 2008: 275-278

[5] Yanjie Liu, Lining Sun and Zhenwei An. An Approach for Generating High Velocity and High Acceleration Trajectories of Industrial Robots, Proceedings of 2005 IEEE International Conference in Robotics and Automation, Espoo, Finland, June 27-30, 2005, pp.199-204.

[6] Gwang-Jo Chung, Doo-Hyung Kim, Hyuk Shin. Structural Analysis of 600Kgf Heavy Duty Handling Robot, Proceedings of 2010 IEEE Conference on Robotics, Automation and Mechatronics, pp.40-45.

[7] Fariborz Behi and Delbert Tesar. Parametric Identification for Industrial Manipulators Using Experimental Modal Analysis. IEEE Transactions on Robotics and Automation, 7(5), 1991, pp. 642-652.

[8] Oguzhan KARHHAN, Zafer BINGUL. Modelling and Identification of STAUBLI RX-60 Robot1, Proceedings of 2008 IEEE International Conference on Robotics, Automation and Mechatronics, pp.78-83

[9] Gwang-Jo Chung, Doo-Hyung Kim, Chan-Hoon Park. Analysis and Design of Heavy Duty Handling Robot, Proceedings of 2008 IEEE International Conference on Robotics, Automation and Mechatronics, pp.774-778.

[10] Chang-Min Ko, Gwang-Jo Chung, Doo-Hyung Kim. Designing of Heavy Duty Handling Robot, Proceedings of the 2009 IEEE International Conference on Mechatronics, Malaga, Spain, April 2009.